Geophysical Journal International

Geophys. J. Int. (2014) **197,** 828–837
Advance Access publication 2014 February 23

doi: 10.1093/gji/ggu038

A statistical simulation of magnetic particle alignment in sediments

David Heslop,[1] Andrew P. Roberts[1] and Rhys Hawkins[1,2]

[1] *Research School of Earth Sciences, The Australian National University, Canberra, ACT* 0200*, Australia. E-mail: david.heslop@anu.edu.au*
[2] *National Computational Infrastructure - VizLab, The Australian National University, Canberra, ACT* 0200*, Australia*

Accepted 2014 January 29. Received 2014 January 19; in original form 2013 August 19

SUMMARY

Sedimentary magnetizations are fundamental to palaeomagnetism, but the mechanisms that control remanence acquisition remain poorly constrained. Observed sedimentary natural remanent magnetizations are often orders of magnitude smaller than the saturation remanent magnetization of the same sediment, which indicates inefficient remanence acquisition. We present a statistical model, based on the von Mises–Fisher distribution, in which magnetic particle reorientations towards an ambient field are considered, without representing the physics of the magnetization acquisition process. The results provide insights into the nature of sedimentary magnetizations. Specifically, an assemblage of randomly oriented magnetic particles can acquire a high-fidelity palaeomagnetic signal with only small rotations (in some cases $<1^{\circ}$) of particles towards the ambient field direction. This demonstrates that the action of a geomagnetic torque on individual magnetic mineral particle orientation may be minor, and that a weak directional bias on an assemblage of particles could be responsible for the typically observed inefficiency of sedimentary remanence acquisition. Additionally, we demonstrate that weak fields produce sedimentary magnetizations with larger directional uncertainties. For natural sediments, however, these uncertainties appear to be small enough to allow reliable recording of directional geomagnetic field behaviour during periods with weak fields, such as palaeomagnetic reversals and excursions.

Key words: Magnetostratigraphy; Palaeointensity; Palaeomagnetic secular variation.

1 INTRODUCTION

After decades of research, sedimentary remanence acquisition remains poorly understood (see Tauxe 1993, 2010; Roberts *et al.* 2013, for reviews). Early conceptual models of the acquisition of sedimentary natural remanent magnetizations (NRMs) were simple; isolated magnetic mineral particles that settle through a still water column experience a geomagnetic torque that rapidly rotates them into alignment with the ambient geomagnetic field (Nagata 1961; Collinson 1965; Nozharov 1966). Once deposited, the magnetic particles form a depositional remanent magnetization (DRM), which provides a record of the contemporary geomagnetic field. When the geomagnetic field strength is high, magnetic particles will align more efficiently and produce larger NRMs. Thus, the direction and strength of a sedimentary NRM can provide essential information concerning the direction and strength of the past geomagnetic field. A detailed early review of sedimentary DRM acquisition was given by Verosub (1977). Numerous studies have, however, identified a multitude of factors that could promote or inhibit magnetic particle rotation in the water column, at the sediment surface and post-depositionally.

During sinking, magnetic particles will be subjected to physical processes, such as rotational Brownian motion (Stacey 1972), fluid torques (Jezek & Gilder 2006; Heslop 2007) and particle flocculation (van Vreumingen 1993a; Katari & Tauxe 2000; Katari & Bloxham 2001; Tauxe *et al.* 2006; Shcherbakov & Sycheva 2008, 2010; Mitra & Tauxe 2009), which are expected to inhibit particle alignment. With a number of simplifying assumptions, these processes can be simulated mathematically to investigate basic scenarios of NRM acquisition, however, the influence of many controlling factors, such as sediment mineralogy, water chemistry and the distribution of particle sizes and shapes, remain poorly constrained (Lu *et al.* 1990; van Vreumingen 1993b; Tauxe *et al.* 2006; Spassov & Valet 2012).

Once deposited onto an unconsolidated sedimentary substrate, magnetic particles will be subjected to a number of processes that will further influence their orientation with respect to the geomagnetic field. For example, particles can be expected to roll and slip on the substrate before coming to rest (King 1955; Griffiths *et al.* 1960). Recent numerical and experimental investigations indicate that systematic offsets between recorded natural sedimentary NRM directions and the expected geomagnetic field direction (e.g. inclination shallowing) could be explained by rolling of magnetic particles at the point of deposition (Jezek *et al.* 2012; Bilardello *et al.* 2013).

After deposition, magnetic particles will still be subjected to processes that influence their alignment with the geomagnetic field. If magnetic particles reside in interstitial voids they remain free to

rotate, tracking the slowing changing geomagnetic field direction until compaction locks them into place to form a post-depositional remanent magnetization (pDRM). The gradual formation and stabilization of the palaeomagnetic signal after deposition can be represented with a lock-in function, which relates burial depth to the proportion of the NRM that is fixed on a geological timescale. The form of such lock-in functions is still under debate (Bleil & von Dobeneck 1999; Roberts & Winklhofer 2004; Suganuma *et al.* 2011; Roberts *et al.* 2013), but must be related to gradual compaction and sediment dewatering (Irving & Major 1964; Kent 1973). Compaction may also introduce systematic biases in the recorded NRM, for example inclination shallowing produced by flattening of elongated magnetic particles into the bedding plane (Blow & Hamilton 1978; Anson & Kodama 1987; Arason & Levi 1990). Other processes, such as bioturbation, also illustrate the complexities involved in NRM acquisition. Bioturbation will randomize particle alignments and might, therefore, be expected to be detrimental to high fidelity NRM acquisition. The action of bioturbation, however, liberates magnetic particles within the unconsolidated sediment and provides an additional opportunity for alignment with the ambient field (Irving & Major 1964; Kent 1973). Thus, an apparently detrimental process may be beneficial to NRM acquisition.

Although our understanding of sedimentary NRM acquisition remains rudimentary, global palaeomagnetic consistency demonstrates that sediments can provide high fidelity palaeomagnetic recording (Tauxe 1993; Guyodo & Valet 1996, 1999; Valet *et al.* 2005; Guyodo & Valet 2006; Channell *et al.* 2009; Ziegler *et al.* 2011; Roberts *et al.* 2013). Early redeposition studies demonstrated that the NRM recording process is inefficient, with the magnitude of sedimentary NRMs far less than their corresponding saturation remanences (Johnson *et al.* 1948; Tauxe 2010). For example, Levi & Banerjee (1976) found that lake sediments carried NRMs with magnitudes corresponding to ∼0.2 per cent of the saturation remanence. Furthermore, using an analysis of synthetic sediment deposition experiments (Anson & Kodama 1987), Arason & Levi (1990) calculated magnetic particle alignment efficiency to be <1 per cent (NRM magnitude compared to the magnetization of a perfectly aligned system). The apparent contradiction between low NRM acquisition efficiencies and high quality sedimentary palaeomagnetic recording requires further investigation. In this study, we present statistical simulations to investigate the extent to which sedimentary magnetic particles must be aligned with an ambient field to produce palaeomagnetic signals similar to those observed in nature (i.e. low-efficiency, but apparently high-fidelity NRMs). We do not consider the relative importance of different DRM and pDRM mechanisms, but instead focus on the extent of particle alignment when all reorientation processes have ceased and a geologically stable NRM is recorded.

2 STATISTICAL MODEL

Numerous recent studies have attempted to quantify and simulate numerically the spectrum of processes that influence NRM acquisition (Katari & Tauxe 2000; Katari & Bloxham 2001; Roberts & Winklhofer 2004; Tauxe *et al.* 2006; Heslop *et al.* 2006; Heslop 2007; Shcherbakov & Sycheva 2008, 2010; Mitra & Tauxe 2009; Jezek *et al.* 2012; Bilardello *et al.* 2013). We do not consider these processes individually, but instead ask what magnitude of particle rotation is required to transform a collection of randomly oriented particles into an ensemble possessing an NRM with the <1 per cent alignment efficiency reported in the literature (Johnson *et al.* 1948; Levi & Banerjee 1976; Arason & Levi 1990; Tauxe 2010). In this way, the factors that control DRM and pDRM acquisition, such as magnetic torque, particle shape, current and fluid resistance, bioturbation and sediment compaction are viewed as components of a single mechanism that controls the ability of a particle assemblage to evolve from a random starting state to a final state that carries useful palaeomagnetic information. The concept of our model is shown in Fig. 1, where an assemblage of unoriented magnetic particles is transformed by individual particle rotations so that the resulting NRM is aligned closely with the ambient field direction.

Earlier studies have considered detailed processes acting on single particles (Jezek & Gilder 2006; Heslop 2007) or ensembles of some hundreds to thousands of particles (Heslop *et al.* 2006; Tauxe *et al.* 2006; Mitra & Tauxe 2009; Jezek *et al.* 2012). Although the assumptions employed in the current model make it less physically realistic than earlier models, the associated simplifications make it feasible for the first time to study large numbers of particles (10^6) within a Monte Carlo framework.

Our simulation is based on collections of unit vectors (i.e. points on the surface of a unit sphere) and the resultant vector they produce in combination. Individual vectors are analogous to single magnetic particles and the resultant vector is the NRM produced by their combined behaviour. The use of unit vectors assumes that each particle has the same remanence intensity, which is clearly an oversimplification of natural systems where magnetic particles span a distribution of sizes and tend to flocculate with non-magnetic particles. For example, Tauxe *et al.* (2006) considered the alignment efficiency of magnetic particles incorporated into flocs and

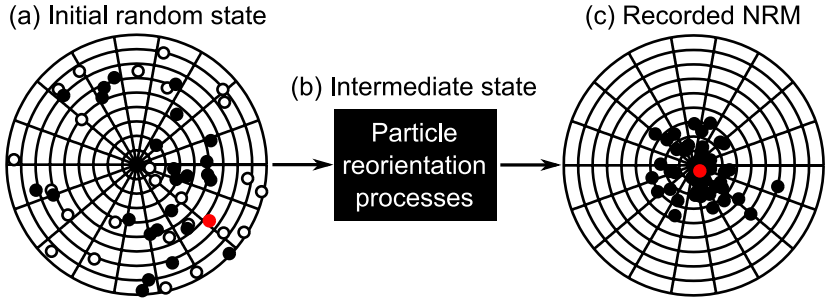

Figure 1. Underlying principle of the statistical model used in this paper. (a) In their initial state, the magnetic moments of individual particles that contribute to a sedimentary magnetization are oriented randomly (black points, with open and closed symbols representing upward and downward inclinations, respectively) and produce a resultant NRM (red point) that is not related to the ambient field (vertical downward). (b) Various processes can give rise to particle reorientations during descent through the water column, at the sediment–water interface or within the sediment column. These processes could promote or inhibit NRM acquisition parallel to the geomagnetic field direction, but it is generally assumed that the geomagnetic field exerts a sufficient control on magnetic particle orientation that the recorded NRM (c) provides a reasonable representation of the ambient geomagnetic field direction.

concluded that a relatively sharp size transition exists between flocs small enough to align readily with the field and flocs too large to reorient under a typical geomagnetic torque. Therefore, Tauxe *et al.* (2006) proposed that the observed total efficiency of the NRM is a balance between aligned and random components. Although our model cannot currently represent the kind of multicomponent processes envisaged by Tauxe *et al.* (2006), it provides a starting point with which to consider the average behaviour of assemblages containing large numbers of magnetic particles.

2.1 Numerical method

In spherical polar coordinates (θ,ϕ), the probability density function of the von Mises–Fisher (vMF) distribution on a 3-D sphere is given by

$$f(\theta, \kappa) = \frac{\kappa}{4\pi \sinh \kappa} \exp(\kappa \cos \theta), \quad (1)$$

where κ is the precision parameter (Fisher 1953). When $\kappa = 0$, the vMF distribution is uniform (i.e. f is constant at all points on the sphere). As κ increases the distribution becomes unimodal with probability concentrated around a colatitude of $\theta = 0^\circ$. Fisher *et al.* (1981) provided an algorithm to generate a pseudo-random point from a vMF distribution with a given nonnegative value of κ, with:

$$\begin{aligned} \lambda &= \exp(-2\kappa), \\ \phi &= 2\pi R_2, \\ \theta &= \begin{cases} \arccos(2R_1 - 1) & \text{if } \kappa = 0, \\ 2 \arcsin \sqrt{\frac{-\log(R_1(1-\lambda)+\lambda)}{2\kappa}} & \text{if } \kappa > 0, \end{cases} \end{aligned} \quad (2)$$

where R_1 and R_2 are random numbers drawn from a uniform distribution in the interval [0,1]. The relationship between R_1 and θ for $\kappa = 0$ is shown in Fig. 2(a).

The algorithm of Fisher *et al.* (1981) can be employed to simulate the orientation of a magnetic particle as it rotates around a great circle towards an ambient field direction (set at $\theta = 0^\circ$). The initial particle orientation is assumed to be independent of the ambient field (i.e. it can lie in any direction) and is generated by drawing values of R_1 and R_2 and setting $\kappa = 0$. With R_1 and R_2 fixed, increasing κ produces orientations along great circles (i.e. constant ϕ) that reach the ambient field direction when $\kappa = \infty$. The rotation of vectors with different R_1 values towards $\theta = 0^\circ$ is shown in Fig. 2(b) as a function of κ. Because R_2 is held constant during the rotation, the ϕ value for each vector remains constant (i.e. ϕ is independent of κ as shown in eq. 2).

The above approach can be extended to consider assemblages of N particles. Drawing N values of R_1 and R_2 with $\kappa = 0$ produces a starting assemblage of orientations that are independent of the ambient field direction. Then as κ is increased, the particle orientations maintain a Fisher distribution while rotating towards the ambient field direction. For any value of κ the resultant of the N unit vectors can be calculated. The orientation and length of this resultant vector are analogous to NRM direction and intensity, respectively.

2.2 Simulation

For a collection of N initial orientations ($\kappa = 0$), constrained numerical optimization (Brent 1973) can be employed to find the value of κ (with R_1 and R_2 fixed) that produces a resultant vector with orientation θ_r. As an example, an NRM may be considered reliable if it is within 5° of the true palaeomagnetic field direction. To simulate this case for an assemblage of initially randomly oriented particles it would be necessary to find the value of κ that yields a resultant vector with $\theta_r = 5^\circ$.

For a given N, the value of κ required to achieve a specific θ_r will depend on the initial orientations produced when $\kappa = 0$. Thus, for given values of N and θ_r, a distribution of κ values exists. This distribution can be sampled using the following Monte Carlo approach.

(i) Select N and θ_r.
(ii) Generate N values of R_1 and R_2.
(iii) Determine (via numerical optimization) the κ value needed to achieve θ_r.
(iv) Calculate the resultant vector length (L_r) for the κ value determined in step (iii).
(v) Calculate the median angle, $\Delta\theta_{50}$, through which the N individual vectors are rotated between $\kappa = 0$ and the κ value determined in step (iii).
(vi) Repeat steps (ii)–(v) for a given number of iterations.

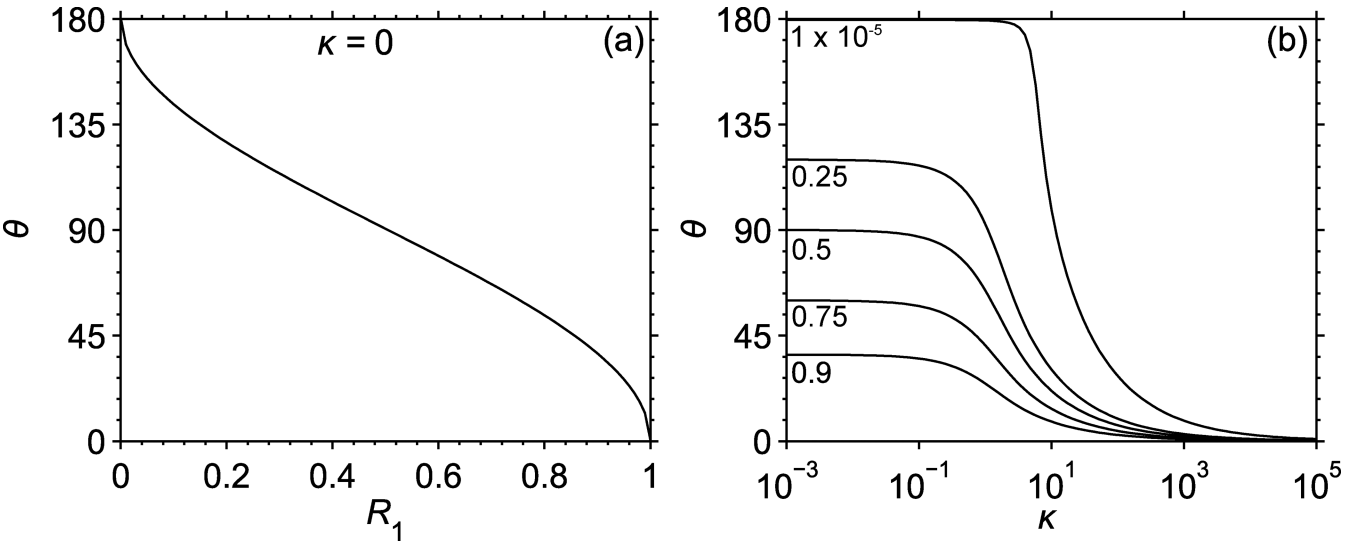

Figure 2. (a) Relationship between R_1 and θ for $\kappa = 0$. (b) Rotation of vectors towards $\theta = 0^\circ$ as a function of κ. The value next to each line corresponds to the R_1 value of that vector, which is held constant so that the vector migrates around a great circle (ϕ fixed) towards $\theta = 0^\circ$.

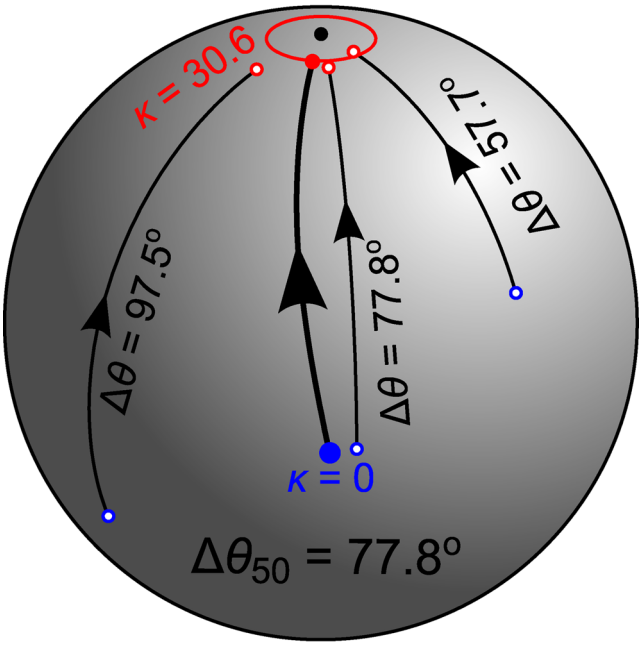

Figure 3. Example particle alignment simulation with $N = 3$. Initial particle orientations (blue open symbols) are drawn randomly (i.e. $\kappa = 0$) from a uniform distribution on the surface of a sphere and the orientation of the resultant vector is calculated (blue closed symbol). Assuming the ambient field direction is at $\theta = 0^\circ$ (black closed symbol), κ is increased so that the individual particles rotate along great circles (thin black lines) towards the field. Once the resultant vector (red closed symbol) achieves a target value of θ_r (red circle) rotation of the individual particles is stopped (red open symbols). The total rotation angle, $\Delta\theta$, is calculated for each particle and the rotation of the assemblage as a whole is represented by the median angle $\Delta\theta_{50}$.

The length calculated in step (iv) is analogous to NRM intensity, whereby imperfect alignment of magnetic particles leads to partial cancellation and a reduced remanence intensity (for $\kappa = \infty$ there would be perfect alignment with $L_r = N$). Step (v) provides a characteristic measure of the particle realignment required to achieve θ_r. For example, $\Delta\theta_{50} = 2^\circ$ indicates that between $\kappa = 0$ and the determined κ value, the median rotation undergone by the N particles is 2°. This procedure is illustrated in Fig. 3.

The largest assemblage that could be considered within a reasonable processing time was $N = 10^6$. An order of magnitude estimate of the number of magnetic particles in a palaeomagnetic sample can be made by simply comparing magnetic particle volume to total sediment volume. For example, consider the case of a cubic sample with sides of 2 cm, a porosity of 70 per cent and a magnetite content of 0.1 per cent by volume. If all the particles in the sample are 100 nm in size (i.e. stable single domain), their abundance would be of the order $N > 10^{12}$. Alternatively, larger pseudo-single domain grains would have abundances of the order of $>10^9$ and $>10^6$ for 1 and 10 μm particles, respectively. Although a natural sediment will contain a spectrum of magnetic particle sizes, it is apparent that N would normally be expected to be orders of magnitude larger than the maximum of $N = 10^6$ employed in our simulations. The implications of this limitation will be discussed below.

NRM acquisition efficiency is represented by the normalized resultant vector length, L_r/N, which can lie between 0 and 1, corresponding to no NRM acquisition (in a perfectly cancelling isotropic magnetic mineral assemblage) and perfect particle alignment, respectively. The L_r/N parameter is analogous to estimating recording efficiency by comparing NRM magnitude to the saturation isothermal remanent magnetization (SIRM), albeit with some important caveats in the case of this simple model. For assemblages with strongly anisotropic alignment, the magnetizing field producing the SIRM should be applied in the same direction as the NRM, which is simple to achieve in the model, but not experimentally. Alternatively, for sufficiently large, isotropically oriented assemblages of uniaxial magnetic particles, 3-D averaging would result in SIRM/$N = 0.5$. In a numerical investigation of NRM formation acquisition, the use of L_r/N circumvents assumptions concerning the degree of anisotropy of SIRMs for a given particle assemblage and is easily interpreted in the context of the model. It is important to note, however, that L_r/N is not a parameter that could be feasibly determined for natural sediments.

3 RESULTS

Two sets of numerical experiments were performed. In the first, we estimated rotations required to align an NRM to within a given angle of the ambient field. In the second, NRM intensities were investigated to quantify how small rotations may influence relative palaeointensity (RPI) estimation.

3.1 NRM alignment

Using the procedure outlined in Section 2.2, distributions of L_r and $\Delta\theta_{50}$ were estimated for θ_r values of 1°, 5° and 10° with logarithmically spaced values of N between 1 and 10^6. For each value of N, 2500 Monte Carlo iterations were performed and the distribution of results is characterized using the median, 5th and 95th percentiles. The median rotations applied to produce a resultant NRM within 10° of the true field direction are shown in Fig. 4(a). Unsurprisingly, as assemblage size increases the required rotation decreases. For example, in the case of assemblages consisting of 10^4 randomly oriented magnetic particles, 95 per cent of the assemblages produce an NRM within 10° of the applied field direction through a median particle reorientation of $\sim 6^\circ$ (Fig. 4a). Similarly for 10^6 particles, 95 per cent of the assemblages require only a median rotation of $\sim 0.6^\circ$ to yield an NRM within 10° of the applied field (Fig. 4a).

The requirement for small rotations for large numbers of magnetic particles is mirrored by the remanence intensity of the final assemblages. Before reorientation, the intensities of the uniformly distributed random orientations follow a Rayleigh distribution (Rayleigh 1919) with the level of mutual cancellation increasing with assemblage size (Heslop 2007). Larger assemblages only require small rotations to produce the desired NRM, therefore, much of the initial cancellation remains and low intensities persist. For example, when $\theta_r = 10^\circ$, 95 per cent of the assemblages with 10^6 particles have final L_r/N values of $\lesssim 0.008$ (Fig. 4b). This magnitude is comparable to measured NRM values with respect to the SIRM for real sediments (e.g. Levi & Banerjee 1976).

Simulation results are shown in Figs 4(c)–(f) for NRMs within 5° and 1° of the applied field direction. As expected, the closer the target NRM is to the applied field direction, the greater the required particle reorientation and the larger the final NRM intensity. For example, as shown above 95 per cent of assemblages with 10^6 particles have a $L_r/N \lesssim 0.008$ when the NRM lies within 10° of the applied field direction. This increases to $L_r/N \lesssim 0.08$ when the NRM is within 1° of the applied field direction (Fig. 4f), as a result of the requirement for greater particle alignment.

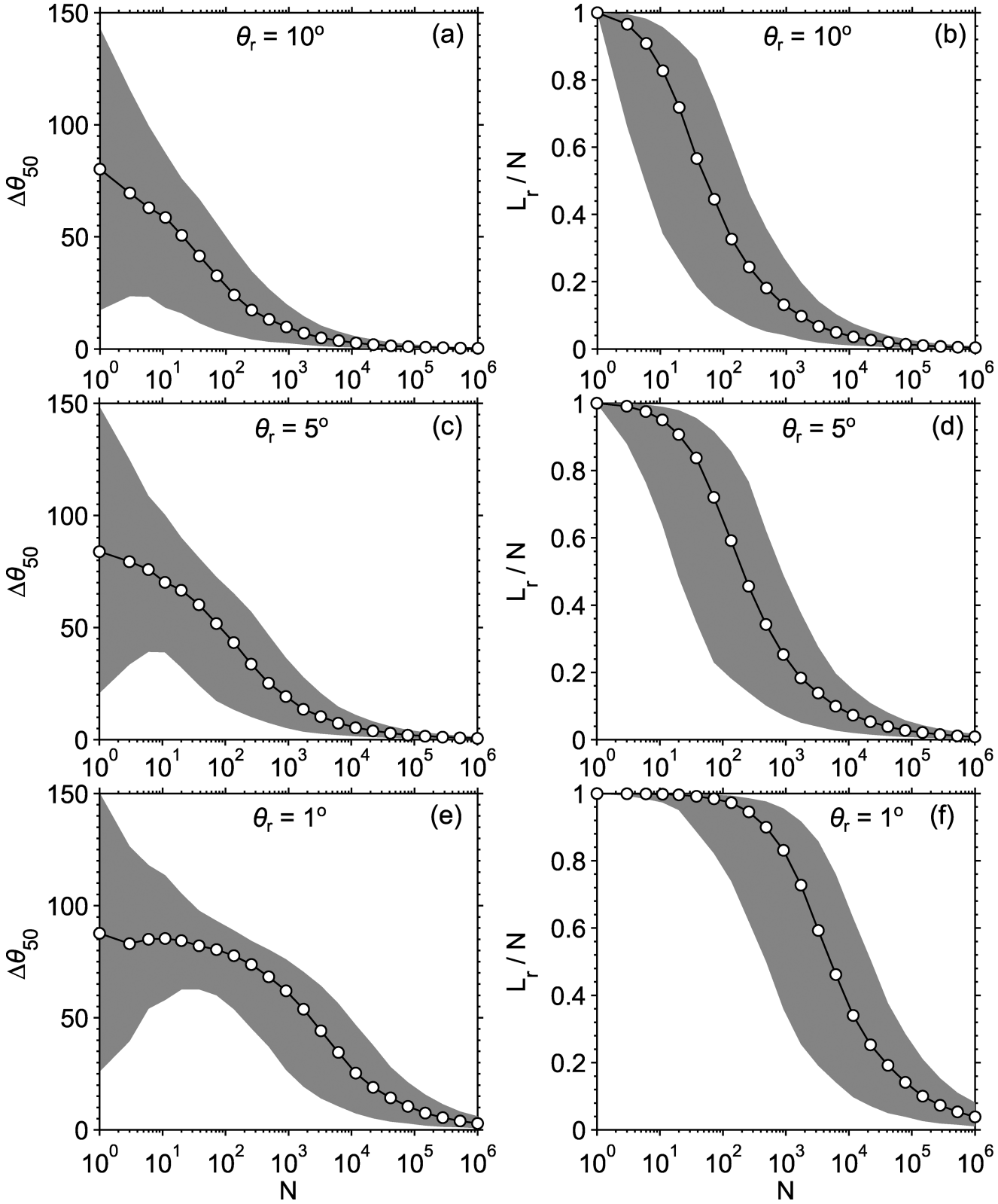

Figure 4. (a) Determination of the median particle rotation angle ($\Delta\theta_{50}$) required to achieve $\theta_r = 10^\circ$ for assemblages ranging in size from 1 to 10^6 particles. The median (open symbols) and 5th (lower limit of shading) and 95th (upper limit of shading) percentiles of 2500 Monte Carlo iterations are shown. (b) Median (line and open symbols) and 5th (lower limit of shading) and 95th (upper limit of shading) percentiles of the resultant vector length at $\theta_r = 10^\circ$. The resultant vector length is normalized by the number of particles in the system (i.e. a value of $L_r/N = 1$ corresponds to perfect mutual alignment of all particles). (c) Same as (a), for $\theta_r = 5^\circ$. (d) Same as (b), for $\theta_r = 5^\circ$. (e) Same as (a), for $\theta_r = 1^\circ$. (f) Same as (b), for $\theta_r = 1^\circ$.

The relationships in Fig. 4 reflect large-scale variations that depend on the number of particles in the assemblage. The plotted results, however, give a false impression of the overall model dependence on N simply because the part of the model space that could be realistically sampled corresponds to $N \leq 10^6$. As discussed above, it is expected that $N \gg 10^6$ for natural sediments with the dependence of $\Delta\theta_{50}$ and L_r/N on N between becoming increasingly flatter as N grows.

3.2 Relative palaeointensity estimation

The underlying assumption of RPI estimation is that stronger ambient fields will align magnetic mineral particles more efficiently and produce larger NRMs (Tauxe 1993). The effect of particle reorientations can be assessed by estimating how L_r/N changes with respect to the median rotation angle ($\Delta\theta_{50}$). Because RPI is estimated under an assumption of direct proportionality (i.e. for a magnetic mineral assemblage with constant composition and concentration, a doubling of NRM intensity is interpreted as a doubling of the ambient field strength), it is most natural to consider relative changes in L_r/N.

An example of our procedure is shown in Fig. 5 for an assemblage with 10^5 vectors. As $\Delta\theta_{50}$ increases, the individual vectors rotate towards the ambient field direction and the magnitude of the normalized resultant vector (L_r/N) increases until a value of 1 is reached (Fig. 5a). To quantify relative changes in L_r/N, a specific point of interest, such as $\theta_r = 1^\circ$, is selected (Fig. 5b). The assemblage specific $\Delta\theta_{50}$ value (and the resulting L_r/N) required to achieve this $\theta_r = 1^\circ$ target is then determined. The L_r/N value is then compared to the value achieved if $\Delta\theta_{50}$ is increased by 1°. The ratio of L_r/N values at $\Delta\theta_{50} + 1^\circ$ and $\Delta\theta_{50}$ provides a relative measure of the increase in normalized intensity when median particle rotation is increased by 1°.

Numerical simulations were performed for assemblages with logarithmically spaced N values between 3 and 10^6. Target values of $\theta_r = 10^\circ$, 5° and 1° were considered for each assemblage and the relative change in L_r/N was estimated for an increase in $\Delta\theta_{50}$ of 1°. For each θ_r value the magnitude of relative growth of L_r/N increases with N (Fig. 6). This results from increased mutual cancellation in larger particle assemblages, where a 1° increase in $\Delta\theta_{50}$ can have a dramatic effect in giving rise to a preferred particle orientation (mirrored by a corresponding reduction in cancellation).

The simulation results demonstrate that sediment NRM magnitude, and thus RPI estimates, can change dramatically with only slight changes in efficiency of particle orientation. The most extreme case in Fig. 6 illustrates this point. For $N = 10^6$ at $\theta_r = 10^\circ$, 95 per cent of the tested assemblages gave rise to intensity increases by a factor of >2.5 when the median particle rotation towards the ambient field direction was increased by 1°. To place this in perspective, Ziegler *et al.* (2011) estimated a Brunhes Chron mean field moment of 6.2×10^{22} Am^2 with a standard deviation of 1.2×10^{22} Am^2. Assuming field strength is approximately normally distributed, the 99th percentile of the moment is located at 9.0×10^{22} Am^2, which is a factor of 1.45 greater than the mean field moment. For a target orientation of $\theta_r = 5^\circ$ (Fig. 6b), >95 per cent of the assemblages with $\sim 3 \times 10^5$ particles would require a $<1^\circ$ increase in $\Delta\theta_{50}$ to produce an intensity change corresponding to a field moment changing from the Brunhes Chron mean to the Brunhes Chron 99th percentile. Similarly ~50 per cent of the assemblages with $\sim 8 \times 10^4$ particles would require a $<1^\circ$ increase in $\Delta\theta_{50}$ to represent the same increase in field moment.

If the difference between NRMs typical of low and high palaeointensities involves particle rotations on the order of $<1^\circ$ there are potentially important implications for RPI reconstruction. Estimates of RPI are based on an assumption of direct proportionality between ambient field strength and NRM corrected for changes in magnetic mineral concentration, while mechanisms that oppose particle alignment are assumed to be constant. If processes that inhibit alignment, for example particle flocculation, change though time, the assumptions of RPI estimation will no longer hold. Given that small changes in particle orientation can lead to large changes in NRM magnitude, the efficiency of processes that inhibit alignment would only need to be modified slightly to yield spurious RPI estimates. The problem of accounting for misaligning processes, such as flocculation, in RPI estimation has been considered in a number of studies, but a satisfactory solution has yet to be found (Tauxe *et al.* 2006; Tauxe & Yamazaki 2007; Hofmann & Fabian 2009).

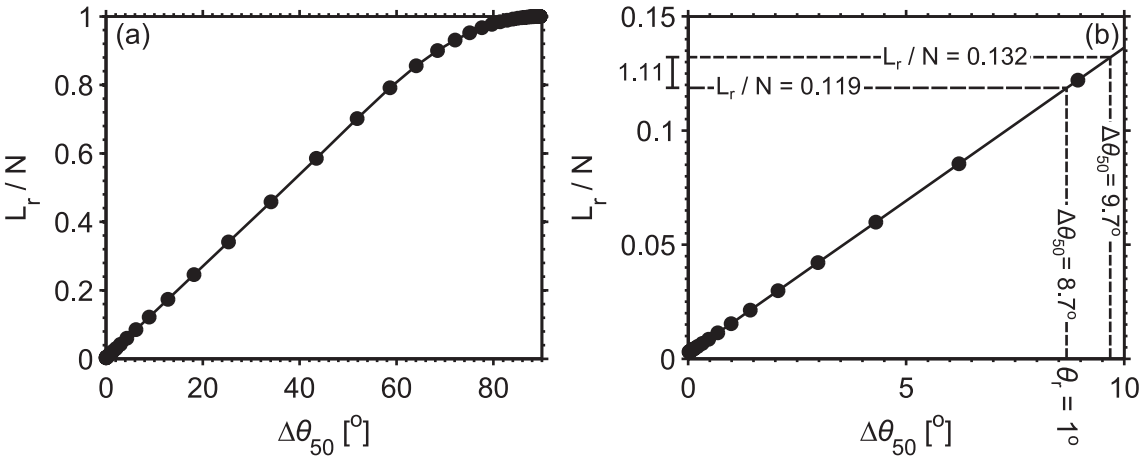

Figure 5. (a) Normalized resultant NRM intensity as a function of $\Delta\theta_{50}$ for an assemblage of $N = 10^5$ vectors. As $\Delta\theta_{50}$ increases the individual vectors are rotated towards the ambient field direction, which results in strong preferred alignment with L_r/N effectively reaching 1 at large values of κ. (b) Enlarged section of (a) for the $\Delta\theta_{50}$ interval [0°, 10°]. The target value of $\theta_r = 1^\circ$ is achieved at $\Delta\theta_{50} = 8.7^\circ$, which corresponds to a L_r/N value of 0.119. If the median particle rotation is increased by 1° to give $\Delta\theta_{50} = 9.7^\circ$, L_r/N becomes 0.132. The ratio of the two intensities is 0.132/0.119 = 1.11, which indicates that for this assemblage an increase in the mean particle rotation of 1° at $\theta_r = 1^\circ$ will produce an 11 per cent increase in L_r/N.

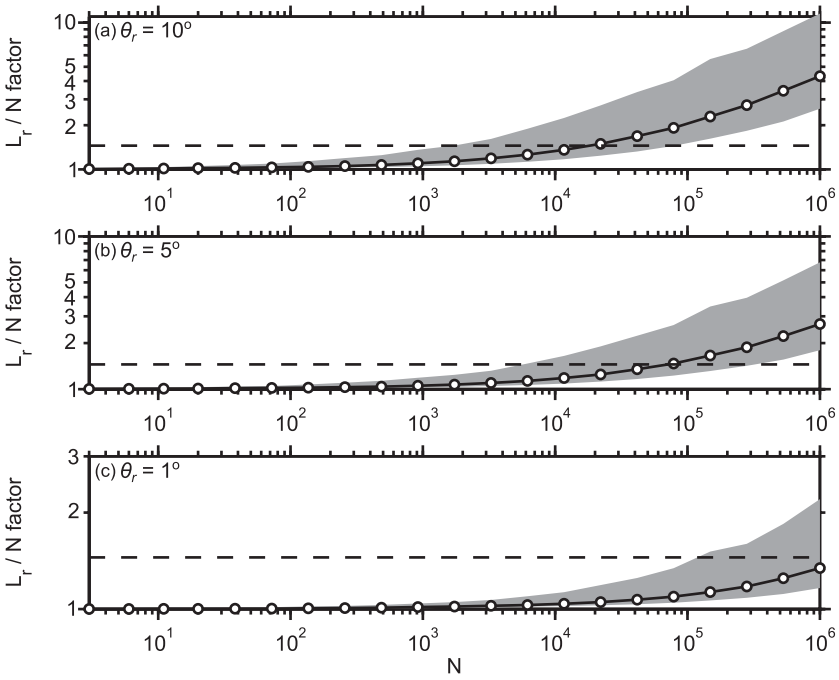

Figure 6. (a) Factors of L_r/N growth between $\Delta\theta_{50}$ and $\Delta\theta_{50}$+1° for $\theta_r = 10°$. The median (open symbols) and 5th (lower limit of shading) and 95th (upper limit of shading) percentiles of 2500 Monte Carlo iterations are shown. The dashed line marks a factor of 1.45, which corresponds to the relative change in intensity between the mean and 99th percentile of the Brunhes Chron field moment distribution (see text for explanation). (b) Same as (a) for $\theta_r = 5°$. (c) Same as (a) for $\theta_r = 1°$.

4 DISCUSSION

Results of our numerical simulations demonstrate how small changes in individual particle orientations can produce large changes in the combined behaviour of an assemblage. For example, in 95 per cent of cases consisting of 10^4 randomly oriented particles, a resultant direction within 5° of the specified field direction can be obtained by a median particle rotation of ∼10°. For larger assemblages (10^6 particles), the same NRM alignment to within 5° of the specified field direction can be obtained with median particle rotations of $\lesssim$1°. Similar behaviour is observed when considering acquisition of RPI signals. For assemblages that contain large numbers of magnetic particles and that record the field direction accurately, it is possible to more than double the NRM magnitude (and hence the RPI estimate) with a median particle rotation <1°.

The small-scale particle realignments needed to produce realistically inefficient NRMs (on the order of 1 per cent alignment) may at first be surprising. The classical representation of sedimentary NRM acquisition involves water-borne magnetic particles oriented with a strong preference towards the ambient field direction (Nagata 1961; Collinson 1965; Nozharov 1966). Numerous subsequent studies have considered misaligning processes that occur in the water column (e.g. flocculation), at the sediment–water interface (e.g. particle rolling) and post-depositionally (e.g. compaction), all of which would inhibit acquisition of a faithful NRM. The importance of these misaligning processes is supported by our calculations, which indicate that sedimentary magnetic particles may only have a small bias towards the ambient field. This bias appears, however, to be sufficiently large to provide high fidelity directional palaeomagnetic recording. This finding is in agreement with the calculations of Arason & Levi (1990), who concluded that sedimentary NRMs are produced by magnetic grains with nearly random orientations. However, the flocculation model of Tauxe *et al.* (2006) explains inefficient NRMs in an alternative manner. Isolated magnetic particles and those incorporated into flocs below a threshold size can readily align with the ambient field to acquire an NRM, while larger flocs remain randomly oriented. This implies that isolated particles and small flocs would have to undergo larger rotations than those indicated by our model to achieve similar NRMs while also compensating for the non-aligned larger flocs.

Comparison of specific values of N (Fig. 4) demonstrates a key relationship between NRM intensity and palaeomagnetic directional uncertainty. For a given assemblage, as individual particles rotate and the resultant NRM migrates towards the ambient field direction, mutual cancellation is reduced (because the particles record a preferred direction) and the NRM intensity increases. For a magnetic mineral assemblage with constant composition, the smaller the value of θ_r (i.e. the error in the recorded NRM direction) the larger the NRM intensity will be. This relationship can be investigated by sampling a vMF distribution with increasing κ values (Fig. 7). High κ values represent strong fields that produce large NRMs with low directional uncertainty. In contrast, low κ values, which correspond to weak fields, produce small NRMs with large directional uncertainty.

If we accept the underlying assumptions of RPI estimation, it is also necessary to accept that the magnitudes of uncertainties associated with NRM directions are related inversely to RPI (Fig. 7). This potentially makes the study of directional field behaviour through palaeomagnetic reversals a challenge because low RPI may imply directions with large errors. An example of this problem is given by considering the extreme case of a sedimentary NRM acquired in the absence of a field. In zero field, magnetic particles will be randomly oriented and mutual cancellation of their magnetizations will be extensive, but not perfect, which will result in a weak NRM. The small

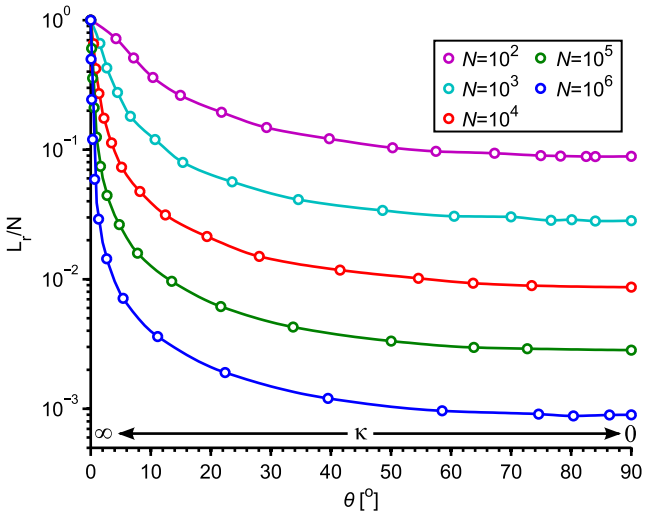

Figure 7. 2500 random samples of size N were drawn from a vMF distribution with a given κ value. Resultant vectors were calculated to provide a distribution of normalized lengths and angular deviations from $\theta = 0^\circ$. The median values of the distributions are plotted to represent the magnitude of the uncertainty of an NRM direction in relation to its intensity. When $\theta = 0^\circ$, the field is strong enough to record a saturated NRM and there is no uncertainty associated with the NRM direction. In contrast, when $\theta = 90^\circ$ the field is so weak that the NRM carries no reliable information concerning field direction even though its intensity is not (quite) zero.

NRM magnitude (and resulting low RPI estimate) would provide useful information concerning the strength of the field (i.e. close to zero), but the measured NRM direction would be meaningless.

To quantify the relationship between RPI estimates and directional uncertainty in our statistical model, we performed an experiment that assumes a directly proportional relationship between ambient field strength and RPI. Assemblages of 10^6 particles were generated with κ values selected to produce $L_r/N = 0.01$. This 1 per cent efficiency is assumed to represent NRM acquisition in a 50 μT field, which corresponds approximately to the Brunhes Chron mean geomagnetic field strength (Ziegler *et al.* 2011). With this assumption, the L_r/N value representing any given ambient field strength (B, in μT) is given by $0.01 \times B/50$. For each particle assemblage, the κ value required to produce a given L_r/N can be estimated numerically and the associated θ value (i.e. the angle between the resultant vector and the field direction) can be determined.

The distribution of θ values between ambient field strengths of 10 and 100 mT assuming a 1 per cent NRM acquisition efficiency at 50 μT is shown in Fig. 8(a). The NRM directional uncertainties are $<10^\circ$ for 95 per cent of the assemblages at 50 μT. By 100 μT this uncertainty is reduced to $<5^\circ$ for 95 per cent of the assemblages. In weaker fields, typical of palaeomagnetic reversals and excursions, the uncertainties increase, reaching up to $<50^\circ$ for 95 per cent of the assemblages at 10 μT. Directional uncertainty is reduced under the assumption of a more efficient NRM acquisition process specified by $L_r/N = 0.05$ in a 50 μT field (Fig. 8b). In such cases of higher NRM acquisition efficiency, the directional uncertainty is reduced as a result of the increased preferential alignment; however, larger uncertainties persist in weak fields.

Our hypothesis of a relationship between RPI and directional uncertainty is in contrast to the acquisition model of Tauxe *et al.* (2006), where it is posited that small flocs will align efficiently with the field. During weak field periods the smallest flocs would still be capable of aligning with the ambient field to produce an NRM with an accurate direction. The cases shown in Fig. 8 were calculated for assemblages of 10^6 particles, as demonstrated above; however, real sediments are expected to have $N \gg 10^6$. As N increases, the uncertainties associated with NRM directions acquired in weak fields will be reduced. Although it is not feasible to sample the model space for $N > 10^6$, it is reasonable to assume that directional uncertainties for large N will be $<5^\circ$ even in weak transitional and excursional fields. Directional uncertainties of this order would be sufficiently small to ensure that sedimentary NRMs carry reliable palaeomagnetic information through weak field periods.

5 CONCLUSIONS

Previously published models that have been developed to investigate sedimentary magnetizations have focused on specific processes that are considered fundamental to NRM acquisition. The underlying physics of many of these processes remains poorly understood. We adopt an alternative statistical strategy that considers the average behaviour of a collection of magnetic particles. The numerous processes that control sedimentary magnetization acquisition are treated as a single mechanism by which randomly oriented magnetic particles are rotated by small amounts to record a preferred alignment with the geomagnetic field vector. The timing of this transformation for any given particle (i.e. in the water column, at

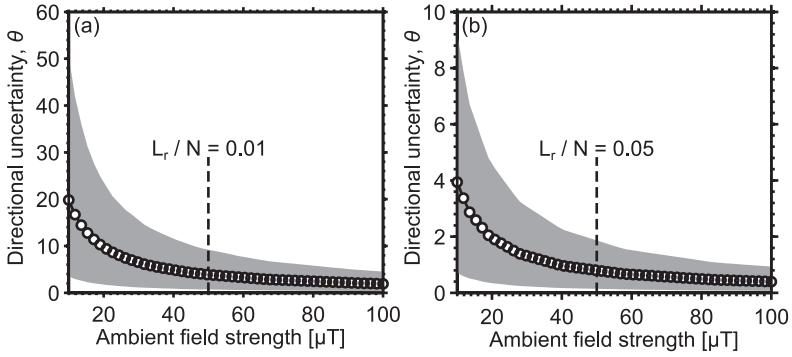

Figure 8. (a) Directional uncertainty estimated for 2500 assemblages composed of 10^6 particles. The assemblages are assumed to achieve $L_r/N = 0.01$ in a 50 μT field, which allows κ to be estimated for any given ambient field strength. For a given assemblage the directional uncertainty (θ) is simply the angle between the resultant vector for the assemblage and the ambient field direction. The median uncertainty is shown by open symbols, and the 5th and 95th percentiles of the uncertainty are shown by the lower and upper limits of the shading, respectively. (b) Same as (a) for a more efficient acquisition system, which achieves $L_r/N = 0.05$ at 50 μT.

the sediment–water interface or within the sediment column) is not specified.

The key insight from our model results is that high-fidelity sedimentary palaeomagnetic directional recording can be achieved with only small rotations of individual magnetic particles. For the large assemblages of magnetic particles that are typical of natural sediments, such rotations may be $\ll 1^\circ$. Thus, for large numbers of magnetic particles it is possible for a sedimentary magnetization to record a direction close to the ambient field direction with an assemblage of particles whose orientations deviate only slightly from a random (i.e. field independent) distribution. It may, therefore, not be necessary to consider geomagnetic torque as the primary or even as a major controller of magnetic particle orientation, but simply as a factor that imparts enough of a bias on the orientation of individual particles to produce high-fidelity palaeomagnetic directional information.

Finally, as a result of imperfect mutual cancellation, a fundamental balance exists between field strength and the fidelity of preserved palaeomagnetic directions. As field strength decreases, mutual cancellation in assemblages of magnetic particles will increase and the estimated RPI will decrease. It is, however, highly improbable that mutual cancellation will be perfect even in the absence of a magnetic field. This means that uncertainties associated with measured palaeomagnetic directions are fundamentally linked to field strength, which may impose a limit on the reliability of geomagnetic information that can be obtained through periods with weak fields, such as polarity transitions and excursions. Directional uncertainty is, however, a function of the number of magnetic particles, which can be exceedingly high in natural sediments. For such systems the directional uncertainty associated with weak field periods is expected to be minor.

ACKNOWLEDGEMENTS

We are grateful for constructive comments from Lisa Tauxe and an anonymous reviewer, which helped to improve the manuscript. This work was supported by the Australian Research Council (grant DP120103952).

REFERENCES

Anson, G.L. & Kodama, K.P., 1987. Compaction-induced shallowing of the post-depositional remanent magnetization in a synthetic sediment, *Geophys. J. R. astr. Soc.,* **88,** 673–692.

Arason, P. & Levi, S., 1990. Models of inclination shallowing during sediment compaction, *J. geophys. Res.,* **95,** 4481–4499.

Bilardello, D., Jezek, J. & Gilder, S., 2013. Numerical simulation of inclination shallowing by rolling and slipping of spherical particles, *Phys. Earth planet. Inter.,* **214,** 1–13.

Bleil, U. & von Dobeneck, T., 1999. Geomagnetic events and relative paleointensity records—clues to high resolution paleomagnetic chronostratigraphies of late Quaternary marine sediments, in *Use of Proxies in Paleoceanography: Examples from the South Atlantic,* pp. 635–654, eds Fisher, G. & Wefer, G., Springer.

Blow, R.A. & Hamilton, N., 1978. Effect of compaction on the acquisition of a detrital remanent magnetization in fine-grained sediments, *Geophys. J. R. astr. Soc.,* **52,** 13–23.

Brent, R.P., 1973. *Algorithms for Minimization Without Derivatives,* Prentice-Hall.

Channell, J. E.T., Xuan, X. & Hodell, D.A., 2009. Stacking paleointensity and oxygen isotope data for the last 1.5 Myr (PISO-1500), *Earth planet. Sci. Lett.,* **283,** 14–23.

Collinson, D.W., 1965. Depositional remanent magnetization in sediments, *J. geophys. Res.,* **70,** 4663–4668.

Fisher, N.I., Lewis, T. & Willcox, M.E., 1981. Tests of discordancy for samples from Fisher's distribution on the sphere, *Appl. Statist.,* **30,** 230–237.

Fisher, R.A., 1953. Dispersion on a sphere, *Proc. R. Soc. Lond.,* **A217,** 295–305.

Griffiths, D.H., King, R.F., Rees, A.I. & Wright, A.E., 1960. Remanent magnetism of some recently varved sediments, *Proc. R. Soc. Lond.,* **A256,** 359–383.

Guyodo, Y. & Valet, J.P., 1996. Relative variations in geomagnetic intensity from sedimentary records: the past 200 thousand years, *Earth planet. Sci. Lett.,* **143,** 23–36.

Guyodo, Y. & Valet, J.P., 1999. Global changes in intensity of the Earth's magnetic field during the past 800 kyr, *Nature,* **399,** 249–252.

Guyodo, Y. & Valet, J.P., 2006. A comparison of relative paleointensity records of the Matuyama Chron for the period 0.75-1.25 Ma, *Phys. Earth planet. Inter.,* **156,** 205–212.

Heslop, D., 2007. Are hydrodynamic shape effects important when modelling the formation of depositional remanent magnetization?, *Geophys. J. Int.,* **171,** 1029–1035.

Heslop, D., Witt, A., Kleiner, T. & Fabian, K., 2006. The role of magnetostatic interactions in sediment suspensions, *Geophys. J. Int.,* **165,** 775–785.

Hofmann, D.I. & Fabian, K., 2009. Correcting relative paleointensity records for variations in sediment composition: results from a South Atlantic stratigraphic network, *Earth planet. Sci. Lett.,* **284,** 34–43.

Irving, E. & Major, A., 1964. Post-depositional detrital remanent magnetization in a synthetic sediment, *Sedimentology,* **3,** 135–143.

Jezek, J. & Gilder, S.A., 2006. Competition of magnetic and hydrodynamic forces on ellipsoidal particles under shear: influence of the Earth's magnetic field on particle alignment in viscous media, *J. geophys. Res.,* **111,** B12S23, doi:10.1029/2006JB004541.

Jezek, J., Gilder, S. & Bilardello, D., 2012. Numerical simulation of inclination shallowing by rolling and slipping of spherical particles, *Comput. Geosci.,* **49,** 270–277.

Johnson, E.A., Murphy, T. & Torreson, O.W., 1948. Pre-history of the Earth's magnetic field, *Terr. Magn. Atmos. Electr.,* **53,** 349–372.

Katari, K. & Bloxham, J., 2001. Effects of sediment aggregate size on DRM intensity: a new theory, *Earth planet. Sci. Lett.,* **186,** 113–122.

Katari, K. & Tauxe, L., 2000. Effects of surface chemistry and flocculation on the intensity of magnetization in redeposited sediments, *Earth planet. Sci. Lett.,* **181,** 489–496.

Kent, D.V., 1973. Post-depositional remanent magnetisation in deep sea sediment, *Nature,* **246,** 32–34.

King, R.F., 1955. The remanent magnetism of artificially deposited sediments, *Mon. Not. R. Astron. Soc. Geophys. Suppl.,* **7,** 115–134.

Levi, S. & Banerjee, S.K., 1976. On the possibility of obtaining relative paleointensities from lake sediments, *Earth planet. Sci. Lett.,* **29,** 219–226.

Lu, R., Banerjee, S. & Marvin, J., 1990. Effects of clay mineralogy and the electric conductivity of water in the acquisition of depositional remanent magnetization in sediments, *J. geophys. Res.,* **95,** 4531–4538.

Mitra, R. & Tauxe, L., 2009. Full vector model for magnetization in sediments, *Earth planet. Sci. Lett.,* **286,** 535–545.

Nagata, T., 1961. *Rock Magnetism,* Maruzen.

Nozharov, P.B., 1966. On the theory of depositional remanent magnetization, *Pure appl. Geophys.,* **64,** 52–58.

Rayleigh, L., 1919. On the problem of random vibrations and random flights in one, two and three dimensions, *Phil. Mag.,* **37,** 321–347.

Roberts, A.P. & Winklhofer, M., 2004. Why are geomagnetic excursions not always recorded in sediments? Constraints from post-depositional remanent magnetization lock-in modelling, *Earth planet. Sci. Lett.,* **227,** 345–359.

Roberts, A.P., Tauxe, L. & Heslop, D., 2013. Magnetic paleointensity stratigraphy and high-resolution Quaternary geochronology: successes and future challenges, *Quat. Sci. Rev.,* **61,** 1–16.

Shcherbakov, V. & Sycheva, N., 2010. On the mechanism of formation of depositional remanent magnetization, *Geochem. Geophys. Geosyst.,* **11,** Q02Z13, doi:10.1029/2009GC002830.

Shcherbakov, V. & Sycheva, N.K., 2008. Flocculation mechanism of the acqusition of remanent magnetization by sedimentary rocks, *Phys. Solid Earth,* **44,** 804–815.

Spassov, S. & Valet, J.P., 2012. Detrital magnetizations from redeposition experiments of different natural sediments, *Earth planet. Sci. Lett.,* **351–352,** 147–157.

Stacey, F.D., 1972. On the role of Brownian motion in the control of DRM of sediments, *Pure appl. Geophys.,* **98,** 139–145.

Suganuma, Y., Okuno, J., Heslop, D., Roberts, A.P., Yamazaki, T. & Yokoyama, Y., 2011. Post-depositional remanent magnetization lock-in for marine sediments deduced from ^{10}Be and paleomagnetic records through the Matuyama-Brunhes boundary, *Earth planet. Sci. Lett.,* **311,** 39–52.

Tauxe, L., 1993. Sedimentary records of relative paleointensity of the geomagnetic field: theory and practice, *Rev. Geophys.,* **31,** 319–354.

Tauxe, L., 2010. *Essentials of Paleomagnetism,* Univ California Press.

Tauxe, L. & Yamazaki, T., 2007. Paleointensities, in *Treatise on Geophysics,* Vol. 5: Geomagnetism, ed. Schubert, G., pp. 509–563, Elsevier.

Tauxe, L., Steindorf, J.L. & Harris, A., 2006. Depositional remanent magnetization: toward an improved theoretical and experimental foundation, *Earth planet. Sci. Lett.,* **244,** 515–529.

Valet, J.P., Meynadier, L. & Guyodo, Y., 2005. Geomagnetic dipole strength and reversal rate over the past two million years, *Nature,* **435,** 802–805.

van Vreumingen, M., 1993a. The magnetization intensity of some artifical suspensions while flocculating in a magnetic field, *Geophys. J. Int.,* **114,** 601–606.

van Vreumingen, M., 1993b. The influence of salinity and flocculation upon the acquisition of remanent magnetization in some artifical sediments, *Geophys. J. Int.,* **114,** 607–614.

Verosub, K.L., 1977. Depositional and post-depositional processes in the magnetization of sediments, *Rev. Geophys. Space Phys.,* **15,** 129–143.

Ziegler, L.B., Constable, C.G., Johnson, C.L. & Tauxe, L., 2011. PADM2M: a penalized maximum likelihood model of the 0-2 Ma palaeomagnetic axial dipole moment, *Geophys. J. Int.,* **184,** 1069–1089.